JCI The Journal of Clinical Investigation

Dual mechanisms for the low plasma levels of truncated apolipoprotein B proteins in familial hypobetalipoproteinemia. Analysis of a new mouse model with a nonsense mutation in the Apob gene.

E Kim, … , P Ambroziak, SG Young

J Clin Invest. 1998;101(6):1468-1477. https://doi.org/10.1172/JCI1122.

Research Article

Familial hypobetalipoproteinemia (FHbeta), a syndrome characterized by low plasma cholesterol levels, is caused by mutations in the apo-B gene that interfere with the synthesis of apo-B100. FHbeta mutations frequently lead to the synthesis of a truncated form of apo-B, which typically is present in plasma at > 5% of the levels of apo-B100. Although many FHbeta mutations have been characterized, the basic mechanisms causing the low plasma levels of truncated apo-B variants have not been defined. We used gene targeting to create a mutant allele that exclusively yields a truncated apo-B, apo-B83. In mice heterozygous for the Apob83 allele, plasma levels and the size and density distribution of apo-B83-containing lipoproteins were strikingly similar to those observed in humans with FHbeta and an apo-B83 mutation. Analysis of mice carrying the Apob83 mutation revealed two mechanisms for the low plasma levels of apo-B83. First, Apob83 mRNA levels and apo-B83 secretion were reduced 76 and 72%, respectively. Second, apo-B83 was removed rapidly from the plasma, compared with apo-B100. This mouse model provides a new level of understanding of FHbeta and adds new insights into apo-B metabolism.

Dual Mechanisms for the Low Plasma Levels of Truncated Apolipoprotein B Proteins in Familial Hypobetalipoproteinemia

Analysis of a New Mouse Model with a Nonsense Mutation in the *Apob* Gene

Edward Kim,*‡§ Candace M. Cham,* Murielle M. Véniant,*‡ Patricia Ambroziak,* and Stephen G. Young*‡§

Gladstone Institute of Cardiovascular Disease; ‡Cardiovascular Research Institute; and §Department of Medicine, University of California, San Francisco, California 94141-9100

Abstract

Familial hypobetalipoproteinemia (FHβ), a syndrome characterized by low plasma cholesterol levels, is caused by mutations in the apo-B gene that interfere with the synthesis of apo-B100. FHβ mutations frequently lead to the synthesis of a truncated form of apo-B, which typically is present in plasma at < 5% of the levels of apo-B100. Although many FHβ mutations have been characterized, the basic mechanisms causing the low plasma levels of truncated apo-B variants have not been defined. We used gene targeting to create a mutant allele that exclusively yields a truncated apo-B, apo-B83. In mice heterozygous for the *Apob*^{83} allele, plasma levels and the size and density distribution of apo-B83–containing lipoproteins were strikingly similar to those observed in humans with FHβ and an apo-B83 mutation. Analysis of mice carrying the *Apob*^{83} mutation revealed two mechanisms for the low plasma levels of apo-B83. First, *Apob*^{83} mRNA levels and apo-B83 secretion were reduced 76 and 72%, respectively. Second, apo-B83 was removed rapidly from the plasma, compared with apo-B100. This mouse model provides a new level of understanding of FHβ and adds new insights into apo-B metabolism. (*J. Clin. Invest.* 1998. 101:1468–1477.) Key words: hypolipidemia • lipoproteins • cholesterol • exencephalus • nonsense mutations • mRNA stability

Introduction

Familial hypobetalipoproteinemia (FHβ)[1] is a relatively common autosomal codominant syndrome characterized by abnormally low plasma concentrations of apo-B and LDL cholesterol (1). The syndrome is caused by mutations in the apo-B gene that interfere with the synthesis of a full-length apo-B100 molecule. Heterozygotes for FHβ typically have LDL cholesterol levels < 40 mg/dl and are asymptomatic. Homozygotes have extremely low LDL cholesterol levels (≤ 5 mg/dl), and the clinical presentation can vary from an absence of symptoms to severe neurological and gastrointestinal dysfunction, depending on the precise nature of the apo-B gene mutation (1). Nearly all of the mutations reported to cause FHβ have been point mutations leading to premature stop codons (1).

In most well-characterized cases of FHβ, a nonsense or frameshift mutation leads to the synthesis of a truncated form of apo-B. The concentration of the truncated apo-B in the plasma is invariably very low, typically < 5% of the concentration of the apo-B100 produced by a normal allele. This is true regardless of whether the truncated apo-B is long enough to form triglyceride-rich lipoproteins (2) or whether it contains the LDL receptor–binding domain (3, 4).

Despite the molecular characterization of many mutations causing FHβ, the mechanism for the low plasma concentrations of truncated apo-B proteins remains obscure (1). Although the low levels of truncated apo-B's in FHβ can only be explained by decreased production or enhanced clearance, definitive data on the basic mechanisms are lacking (1). Several lipoprotein kinetics studies in human subjects with truncated apo-B's have suggested enhanced lipoprotein clearance (3, 5–8), whereas others have suggested reduced synthesis of lipoproteins (9–11). Unfortunately, kinetics studies with exogenously or endogenously labeled lipoproteins depend on a number of metabolic assumptions, and data from these experiments cannot be extrapolated to infer the actual rates of apo-B synthesis and secretion from cells (12).

In recent years, several groups have used gene targeting in embryonic stem (ES) cells to generate mice carrying modified apo-B alleles (13–16), but for several reasons, none serves as a faithful model of human FHβ. Homanics et al. (13) used gene targeting in mouse ES cells to generate a mutant allele that yielded a truncated apo-B, apo-B70, as well as apo-B48. Unlike the typical mutations causing human FHβ, the apo-B70 mutation introduced a large insertion that affected the structure of the apo-B mRNA. Not surprisingly, the level of this structurally abnormal transcript was low. More recently, our laboratory used gene targeting to replace the apo-B48–editing codon (codon 2153) of the apo-B gene with a stop codon (15), thereby generating apo-B48–only mice. These animals had normal levels of the mutant apo-B mRNA, and their plasma apo-B48 levels were actually higher than those in wild-type mice (15). Once again, however, the utility of the apo-B48–only mice as a model of FHβ is questionable because the normal mRNA levels produced by this mutant allele might simply reflect the fact that the nonsense mutation was placed into a natural site.

To create an appropriate model of human FHβ and to gain new and definitive insights into basic mechanisms of the disorder, we used gene targeting in mouse ES cells to insert a subtle

Address correspondence to Edward Kim, M.D., Gladstone Institute of Cardiovascular Disease, P.O. Box 419100, San Francisco, CA 94141-9100. Phone: 415-826-7500, FAX: 415-285-5632.

Received for publication 7 July 1997 and accepted in revised form 22 January 1998.

1. *Abbreviations used in this paper:* ES, embryonic stem; FHβ, familial hypobetalipoproteinemia; FPLC, fast-performance liquid chromatography; IDL, intermediary density lipoproteins; p.c., post coitus.

J. Clin. Invest.

0021-9738/98/03/1468/10 $2.00
Volume 101, Number 6, March 1998, 1468–1477
http://www.jci.org

mutation (Leu3798Stop) into the mouse apo-B gene, generating mice that make a truncated apo-B, apo-B83. Here, we demonstrate that these new gene-targeted mice serve as an appropriate model for studying human FHβ, and we use this model to obtain definitive data regarding the metabolic basis of FHβ.

Methods

Generation of heterozygous apo-B83–only (Apob$^{83/+}$) *mice.* A sequence-insertion gene-targeting vector (see Fig. 1) was constructed from strain B10.A mouse *Apob* clones 15A5M and 15A6 (15). Clone 15A5M begins 55 bp past the beginning of exon 26 and extends to a SacI site at the 3′ end of exon 26 (6540 bp into exon 26). The clone contains a CTA (Leu) missense mutation at the site of the apo-B mRNA–editing codon (codon 2153), which prevents the apo-B mRNA–editing reaction from generating a premature stop codon. The CTA missense mutation is tagged with a new HindIII site (15). Clone 15A6 starts at the SacI site at the 3′ end of exon 26 and extends to an EcoRI site 1.2 kb downstream from the polyadenylation signal of the apo-B gene. Site-directed mutagenesis with the oligonucleotide 5′–GGGTGACACTAGTCTAGTCAACATC–3′ (primer B83Stop-Spe) was used to insert a nonsense mutation into clone 15A6 (generating clone 15A6M). This mutation changed a CTG (Leu) in exon 26 (corresponding to human apo-B100 amino acid 3,798) to the stop codon TAG (a Leu3798Stop mutation) and introduced a new SpeI site into the gene. To construct the gene-targeting vector, the 6-kb insert of p15A5M was removed with SacI and SalI and directionally ligated into the SalI and SacI sites of p15A6M. Subsequently, a neomycin resistance gene (*neo*) driven by an RNA polymerase II promoter was inserted into the polylinker SalI site. The vector was then linearized at a unique SauI site (608 bp into mouse exon 26) and electroporated into RF8 ES cells. Targeted clones were identified by Southern blot analysis of both HindIII- and SpeI-digested genomic DNA with a probe located 5′ to the sequences contained in the targeting vector. The probe spanned from intron 24 to exon 25 of the apo-B gene.

Targeted ES cells were microinjected into C57BL/6 blastocysts to generate male chimeric mice (17), and the chimeras were bred with C57BL/6 females to generate heterozygous apo-B83–only mice (*Apob*$^{83/+}$). The *Apob*$^{83/+}$ mice were intercrossed to generate homozygotes and were bred with apo-B100–only mice (*Apob*$^{100/100}$) to generate *Apob*$^{83/100}$ mice. The *Apob*$^{100/100}$ mice were created earlier with a gene-targeting vector that lacked the nonsense mutation at codon 3,798 but was otherwise identical to the apo-B83–only gene-targeting vector (15). All mice used in this study were weaned at 21 d of age and fed a chow diet containing 4.5% fat (Ralston Purina Co., St. Louis, MO).

Generation of Apob$^{83/100}$Apoe$^{-/-}$ *and* Apob$^{83/100}$Ldlr$^{-/-}$ *mice.* *Apob*$^{83/+}$ mice were crossed with *Apoe*$^{-/-}$ (18, 19) and *Ldlr*$^{-/-}$ (20) mice to generate *Apob*$^{83/+}$*Apoe*$^{+/-}$ and *Apob*$^{83/+}$*Ldlr*$^{+/-}$ mice. *Apob*$^{83/+}$ *Apoe*$^{+/-}$ were then crossed with *Apob*$^{100/100}$*Apoe*$^{-/-}$ mice to generate *Apob*$^{83/100}$*Apoe*$^{-/-}$ offspring. *Apob*$^{83/+}$*Ldlr*$^{+/-}$ mice were crossed with *Apob*$^{100/100}$*Ldlr*$^{-/-}$ mice to generate *Apob*$^{83/100}$*Apoe*$^{-/-}$ offspring. *Apoe* and *Ldlr* genotyping was performed by Southern blot and PCR analysis of tail DNA.

Lipoprotein fractionation and Western blot detection of apo-B. VLDL fractions were prepared from mouse plasma samples by ultracentrifugation. Plasma was also size-fractionated by fast-performance liquid chromatography (FPLC) (21). Apo-B in the plasma or lipoprotein fractions was detected by Western blots as described previously (21). The intensity of the bands was quantified with a GS300 transmittance/reflectance scanning densitometer and the GS-365 data system for densitometer (Hoefer Scientific Instruments, San Francisco, CA). Levels of radioactivity within protein bands were determined with a PhosphorImager (Fuji Bio-Imaging Analyzer, BAS 1000 with MacBAS; Fuji Medical Systems, USA, Inc., Stamford, CT). For some experiments, we used fresh plasma from the proband of the apo-B83 kindred, a kindred with FHβ that we analyzed previously in association with Dr. A. Garg and Dr. S. Grundy (University of Texas Southwestern Medical Center, Dallas, TX) (22). To detect human apo-B on Western blots, we used the human apo-B–specific monoclonal antibodies 1D1 or C1.4 (23, 24).

A specific radioimmunoassay for mouse apo-B100. To measure the concentration of apo-B100 in mouse plasma, we used a sandwich radioimmunoassay using two different mouse apo-B100–specific monoclonal antibodies, LF3 and LF5.[2] The assay for mouse apo-B100 is essentially identical to the sandwich assay that we have used extensively to measure human apo-B100 (25–28), except that different monoclonal antibodies were used. Antibody LF5 was used to coat 96-well polyvinylchloride plates, and ^{125}I-LF3 (400,000 cpm per well) was used to detect mouse apo-B100. The background binding ^{125}I-LF3 in the absence of mouse apo-B100 was virtually absent; the assay did not detect any mouse apo-B in the plasma of human apo-B transgenic mice lacking mouse apo-B (29) or in the plasma of apo-E–deficient apo-B48–only mice (30).

Amplification of a cDNA fragment for primer extension analysis. To quantify the relative proportions of transcripts from the two different apo-B alleles in the liver, intestine, and yolk sac of *Apob*$^{83/+}$ or *Apob*$^{83/100}$ mice, a primer extension assay was used, as outlined below. To obtain the template for the primer extension assay, reverse transcription (RT)–PCR was used to amplify a segment of the apo-B transcript. Total RNA from the liver, yolk sac, and intestine of *Apob*$^{83/+}$ and *Apob*$^{83/100}$ mice was isolated with the RNA STAT-60 kit. The first strand of cDNA was synthesized from 5.0 μg of total RNA with an RT-PCR Kit (Stratagene, Inc., La Jolla, CA) and a specific primer corresponding to sequences in exon 28 of the mouse *Apob* gene (5′–AGGTGAGCCTCTCCCTGCCAGTCC–3′ [primer 8400bottom]). The cDNA was amplified with *Taq* polymerase (Boehringer Mannheim Biochemicals, Indianapolis, IN), oligonucleotide primer 8400bottom, and a second oligonucleotide located in exon 26 (5′–GCCTCAACCTAACAATGCTCCCC–3′ [primer 7191top]).

Primer extension assay. The primer extension assay was designed to quantify the relative proportions of transcripts from the two different alleles in *Apob*$^{83/+}$ and *Apob*$^{83/100}$ mice. Briefly, a labeled oligonucleotide located immediately downstream from the apo-B83 nonsense mutation was annealed to the amplified cDNA template and extended in the presence of dideoxy-TTP. Because of the nonsense mutation in the *Apob*^{83} allele, the primer extension product from the *Apob*^{83} cDNA was 28 bp in length versus 33 bp for the *Apob*$^{+}$ or *Apob*^{100} cDNA. After size-fractionated by electrophoresis on an 8% polyacrylamide gel containing 7.5 M urea and 1 × TBE, gels were then dried and exposed to autoradiographic film. The radioactivity in each band was quantified using the AMBIS radioanalytic imaging system (San Diego, CA). For data analysis, all values are expressed as mean±SEM. A *t* test was used for statistical comparisons.

Analysis of pre-mRNA. The primer extension assay was designed to quantify the relative proportions of apo-B pre-mRNA from the two different alleles in *Apob*$^{83/+}$ and *Apob*$^{83/100}$ mice. For these experiments, 5.0 μg of liver RNA was treated with 2 U of DNase I (RNase free; Boehringer Mannheim Biochemicals) for 30 min at 37°C. After the DNase was heat inactivated, the first strand of cDNA was synthesized with the RT-PCR Kit (Stratagene, Inc.) and an intron 26–specific primer (5′–GAACTCAGTTGGAATAACATAGTATC–3′ [primer in26bottom]). Subsequently, a segment of cDNA was amplified with *Taq* polymerase and oligonucleotides primer

2. Mouse monoclonal antibodies specific for mouse apo-B100 were generated in apo-B48-only mice that had been immunized with apo-B100 (Flynn, L., C. Huffine, and S. Young, manuscript in preparation). Both of the mouse monoclonal antibodies used in the RIA bind downstream from the carboxyl terminus of apo-B83.

in26bottom and primer 7191top. The PCR product was 507 bp. To determine if the RNA sample contained small amounts of genomic DNA despite DNase treatment, control PCR reactions were performed with RNA samples that had not undergone the reverse transcriptase step.

Isolation of primary hepatocytes from mouse liver. Primary mouse hepatocytes were prepared using a protocol similar to one described for isolating primary rat hepatocytes (31). The mice were anesthetized with ethyl ether, and a cannula was inserted into the inferior vena cava via the right atrium. The liver was retrogradely perfused with liver perfusion medium (Life Technologies, Gaithersburg, MD) and then collagenase-lipase medium (Life Technologies). The perfusate was drained through an incision in the portal vein. The digested liver was then removed, minced with iris scissors, and dispersed by pipetting up and down several times. The cell suspension was filtered through sterile gauze and centrifuged at 60 *g*. Hepatocytes were then resuspended in hepatocyte wash medium (Life Technologies) and pelleted by centrifugation at 60 *g*. After three wash cycles, 6.4×10^5 cells were plated in each well of six-well plates coated with rat tail collagen type I and incubated at 37°C under 5% CO_2 with 2 ml of culture medium consisting of DME (with glucose [4500 mg/liter]; with $NaHCO_3$; without methionine, cysteine, and glutamine [Sigma, St. Louis, MO]) supplemented with 1% (vol/vol) 200 mM glutamine, 2.5% (vol/vol) 100 mM sodium pyruvate, 1% (vol/vol) 10 mM nonessential amino acids, and 6.5% (vol/vol) FBS (Life Technologies). Hepatocytes were then used for either RNA stability studies or metabolic labeling experiments (see below).

Metabolic labeling experiments with primary hepatocytes. 2 h after hepatocytes were plated (see above), 50 μl of Pro-mix (530 MBq/ml; Amersham Corp., Arlington Heights, IL), an L-[^{35}S]methionine labeling solution, was added to each well. After a 3-h incubation at 37°C, the medium was collected. The cells were washed three times with PBS (Digene Corp., Beltsville, MD), harvested, and disrupted by sonication for 10 s in a model 400 sonifier (duty cycle constant, output control 0.3; Branson Ultrasonics Corp., Danbury, CT). The relative amounts of apo-B83 and apo-B100 in cells were determined by immunoprecipitating the apo-B with a mouse apo-B–specific antiserum (21) and then size-fractionating the immune complexes on an SDS-polyacrylamide gel (32). Dried gels were then analyzed with a PhosphorImager.

The apo-B–containing lipoproteins secreted into the primary hepatocyte medium were separated by discontinuous sucrose gradient ultracentrifugation (32). Gradients were unloaded into eight fractions, and apo-B was precipitated from each fraction with a mouse apo-B–specific antiserum (21), according to published immunoprecipitation protocols (32). Once again, the immune complexes were analyzed by SDS-PAGE and PhosphorImager and scanning densitometer analysis.

Inhibition of lipoprotein clearance in Apob$^{83/100}$ mice. Triton WR-1339 (Tyloxapol, 20% stock solution in PBS [vol/vol]; Sigma Chemical Co.) at a dose of 500 mg/kg of body weight was injected directly into the jugular veins of anesthetized *Apob*$^{83/100}$ mice using an insulin syringe. This detergent has been shown to block lipoprotein clearance (33). Mice were bled from the retroorbital plexus before Triton WR-1339 injection and several time points after injection. Levels of apo-B83 compared with apo-B100 were assessed by Western blot analysis as described earlier.

Examination of mouse embryos. Timed matings were established as described previously (14, 34). Pregnant females were killed on days 10.5, 12.5, 14.5–16.5, 18.5, and 20.5 post coitus (p.c.). After dissection of the embryo and fetal membranes from the uterus, portions of the fetal membranes or embryos were fixed in 3% paraformaldehyde or used for DNA/RNA isolation. Fixed tissues were sectioned, stained with hematoxylin and eosin, and examined by light microscopy.

Results

Generation of heterozygous apo-B83–only mice. To generate a mouse model of human FHβ associated with a truncated apo-B, we used a sequence-insertion gene-targeting vector (Fig. 1) to insert two subtle mutations into exon 26 of the mouse apo-B gene. The first mutation, Leu3798Stop, was a point mutation typical of those causing FHβ in humans and was predicted to yield a truncated apo-B protein, apo-B83. The second mutation was a CTA-missense mutation in the apo-B mRNA–editing codon (codon 2,153) that prevented the apo-B mRNA–editing machinery from generating a stop codon, thereby abrogating the formation of apo-B48. Eliminating apo-B48 synthesis is essential for creating a mouse model of human FHβ because mouse liver possesses apo-B mRNA–editing activity and produces a substantial amount of apo-B48, whereas the human liver lacks editing activity and synthesizes no apo-B48. Previously, we used the same CTA-missense mutation to generate gene-targeted mice that synthesize exclusively apo-B100 (apo-B100–only mice), and estab-

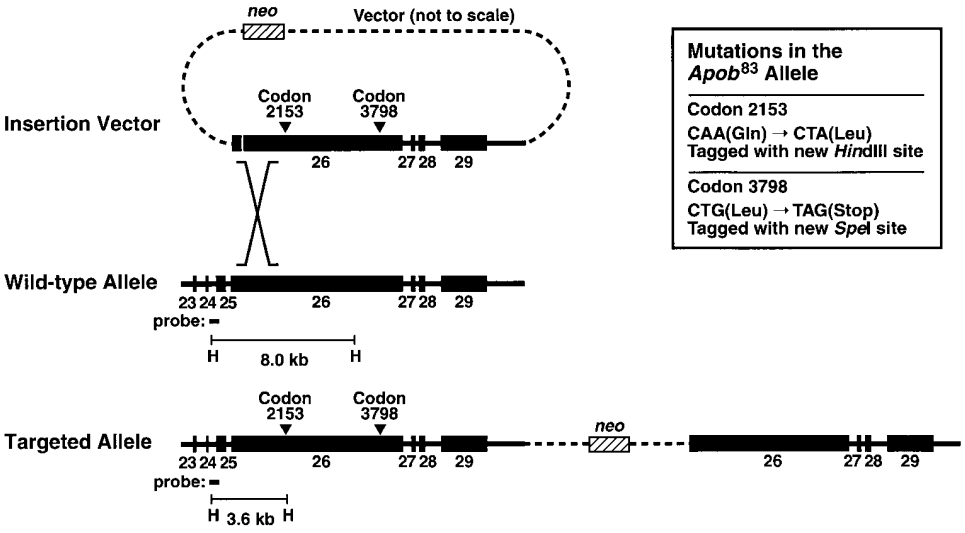

Figure 1. Diagram of the apo-B83 gene–targeting vector, the mouse apo-B gene, and a targeted *Apob*^{83} allele. The gene-targeting vector contained a nonsense mutation (and a new SpeI site) in the 3′ portion of exon 26 (*Codon 3798*). In addition, to eliminate apo-B48 production from the mutant allele, codon 2153 (the apo-B48–editing site) was changed from CAA to CTA. This latter mutation was tagged with a new HindIII site.

lished that the CTA-missense mutation eliminates apo-B48 production without affecting intestinal or hepatic apo-B mRNA levels (15).

The apo-B83 gene-targeting vector was electroporated in ES cells, and two targeted clones were identified (from a total of 196) by Southern blot analysis of HindIII-digested genomic DNA. This screening strategy identified ES cell clones containing the CTA-missense mutation at residue 2,153 (which is tagged by a new HindIII site) (Fig. 1). Subsequent Southern blotting of SpeI-digested genomic DNA with the same probe revealed that both targeted ES cell clones contained a new SpeI site at the 3′ end of exon 26, indicating that both clones also contained the nonsense mutation. Both ES cell clones were used to generate high-percentage male chimeric mice, which were bred with C57BL/6 females. All chimeras from both ES cell lines transmitted the targeted mutation to their progeny, generating heterozygous apo-B83–only ($Apob^{83/+}$) mice. These mice developed normally, and both males and females were healthy and fertile. However, the homozygous mice ($Apob^{83/83}$) manifested severe developmental abnormalities, and only several live animals were born (see analysis below). The phenotypes of $Apob^{83/+}$ derived from the two targeted ES cell clones were identical. Likewise, the phenotypes of $Apob^{83/83}$ mice derived from the two targeted ES cell clones were identical.

Generation and analysis of Apob$^{83/100}$ *mice.* The $Apob^{83/+}$ mice were mated with $Apob^{100/100}$ mice (15) to generate $Apob^{83/100}$ mice. By Western blot analysis, apo-B83 was virtually undetectable in the plasma of the $Apob^{83/100}$ mice, but the $Apob^{83/100}$ mice could nevertheless be distinguished from the $Apob^{100/+}$ mice because the plasma of the $Apob^{83/100}$ mice lacked apo-B48 (and had relatively low levels of apo-B100) (Fig. 2).

In subsequent experiments, we were able to identify very small amounts of apo-B83 in the plasma of mice fed a chow diet ad libitum, but apo-B83 was consistently undetectable in mice after a 4-h fast (data not shown). In contrast, apo-B83 was readily detectable in the VLDL of $Apob^{83/100}$ mice (Fig. 3), reflecting this fraction's enrichment in apo-B83. In the VLDL, the ratio of apo-B83 to apo-B100 was 10:1 (see Fig. 3 legend).

Remarkably, the relative amounts of apo-B83 and apo-B100 in the VLDL of the $Apob^{83/100}$ mice appeared to be identical to those in the VLDL of a human subject who was heterozygous for an apo-B83 mutation (22) (Fig. 3). In this human apo-B83 heterozygote, apo-B83 was virtually undetectable in the plasma but was easily detectable in the VLDL. (Previously, we showed that apo-B83 was easily detectable in the VLDL fraction of human apo-B83 heterozygotes, but was undetectable in the LDL, even on a silver-stained SDS-polyacrylamide gel; reference 22.) When plasma from $Apob^{83/100}$ mice was size-fractionated on an FPLC column, apo-B83 could be clearly identified only in the first of the VLDL fractions (Fig. 4). In contrast, most of the mouse apo-B100 was located within LDL-sized particles. In the human sample, apo-B83 and apo-B48 were easily identified in the first of the three VLDL fractions, and only a trace of apo-B83 and apo-B48 were found in the intermediary density lipoproteins (IDL)/LDL fractions, where the vast majority of the apo-B100 was located (data not

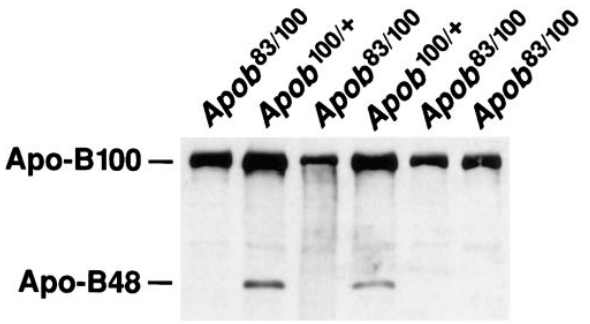

Figure 2. Western blot analysis of the plasma from $Apob^{83/100}$ and $Apob^{100/+}$ mice. Apo-B48 was present in the plasma of $Apob^{100/+}$ mice but was absent in the plasma of $Apob^{83/100}$ mice; the concentration of apo-B100 was lower in the $Apob^{83/100}$ mice than in the $Apob^{100/+}$ mice.

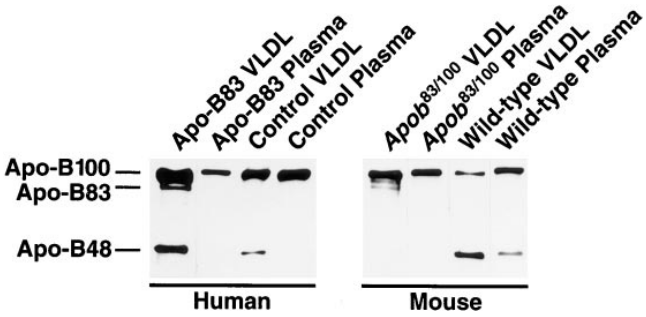

Figure 3. Western blot analysis of VLDL and plasma from $Apob^{83/100}$ mice and from a human subject who was heterozygous for an apo-B83 mutation. The human VLDL sample was prepared from plasma obtained after an overnight fast. Mouse VLDL was prepared from plasma pooled from four $Apob^{83/100}$ mice that had been fasted for 4 h. By scanning densitometer, the ratio of apo-B83 to apo-B100 in the human apo-B83 heterozygote was 1:5.5, and it was 1:10 in the VLDL of the $Apob^{83/100}$ mice. Similar results were obtained with PhosphorImager analysis.

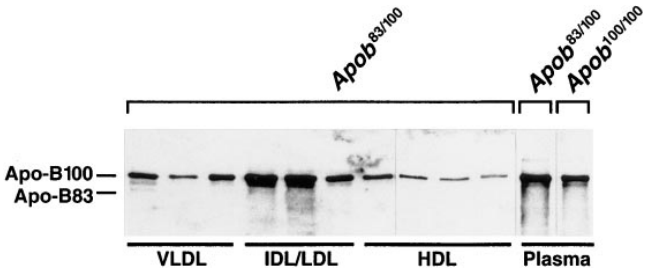

Figure 4. Distribution of apo-B proteins in the plasma of $Apob^{83/100}$ mice. Plasma from mice was size-fractionated by FPLC. Consecutive fractions were then pooled and analyzed by a Western blot of an SDS-polyacrylamide gel. Apo-B83 was clearly identifiable only in the first of the three VLDL fractions. The ratio of apo-B83 to apo-B100 in the first of the three VLDL fractions was 1:9, yet only 16% of the apo-B100 was located in the VLDL fractions. We therefore estimate that the concentration of apo-B83 in the whole plasma of the $Apob^{83/100}$ mice was $\sim$ 2% of that of apo-B100. The intensities of apo-B83 and apo-B100 bands were quantified with a PhosphorImager. When the plasma from the human apo-B83 heterozygote was analyzed by FPLC, virtually identical results were obtained (data not shown).

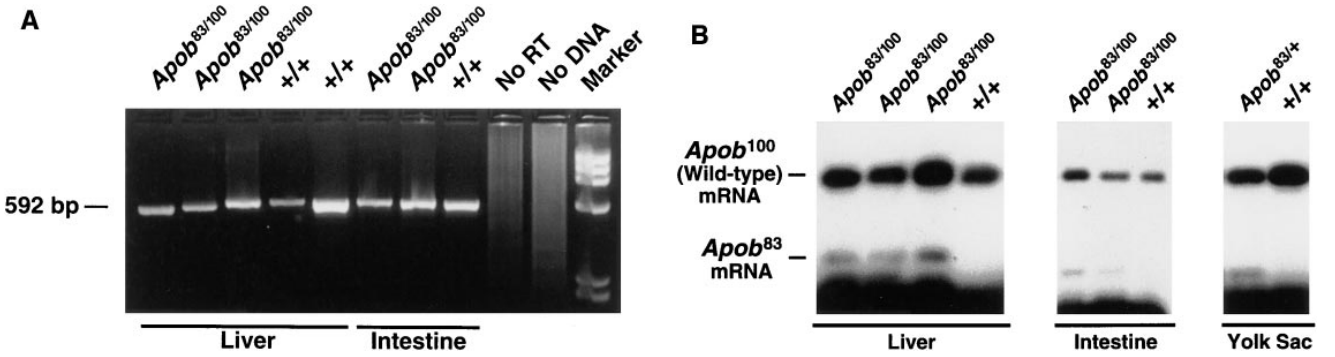

Figure 5. Primer extension analysis of the steady state levels of *Apob*^{83} mRNA. (*A*) RT-PCR reactions demonstrating the enzymatic amplification of a 592-bp fragment of the apo-B cDNA from *Apob*$^{83/100}$ mice with oligonucleotide primers homologous to sequences within exons 26 and 28 of the apo-B gene. Identical results were obtained with yolk sac RNA. (*B*) Primer extension assay of the RT-PCR products from *Apob*$^{83/100}$ mice. With an *Apob*^{100} (or *Apob*$^{+}$) allele, the product of the primer extension reaction is 33 bp, whereas it is 28 bp for the *Apob*^{83} allele. Identical results were obtained with cDNA amplified from livers, yolk sacs, and intestines of *Apob*$^{83/+}$ mice.

shown). The striking similarity in the amount of apo-B83 in the plasma of the *Apob*$^{83/100}$ mice and the plasma of the human apo-B83 heterozygote, along with the striking similarity in the size and density distribution of human and mouse apo-B83, strongly suggests that the *Apob*$^{83/100}$ mice are a useful model for studying mechanisms of human FHβ.

Cholesterol and apo-B100 levels in Apob$^{83/100}$ *and Apob*$^{100/100}$ *mice.* The mean total plasma cholesterol level was lower in female *Apob*$^{83/100}$ mice (n = 8) than in age- and sex-matched *Apob*$^{100/100}$ mice (n = 5) (26.9±2.4 mg/dl versus 45.6±3.0 mg/dl; P = 0.0005). We measured mouse apo-B100 levels in *Apob*$^{83/100}$ and *Apob*$^{100/100}$ mice using a monoclonal antibody-based RIA. The plasma levels of apo-B100 in *Apob*$^{83/100}$ mice were 36% of those in *Apob*$^{100/100}$ mice (2,402±68 cpm versus 8,671±830 cpm, respectively; $P < 0.002$). Thus, the amount of apo-B100 in the *Apob*$^{83/100}$ mice was less than half of that in the *Apob*$^{100/100}$ mice. A less-than-half-normal amount of apo-B100 is very frequently found in human FHβ (1).

The Apob^{83} *allele is associated with low levels of apo-B mRNA.* To determine if the *Apob*^{83} allele produced normal levels of the apo-B mRNA and to determine if the apo-B transcript was of normal length, we used Northern blots to examine the RNA from yolk sacs of 15-d *Apob*$^{83/83}$ and wild-type embryos. Both wild-type and *Apob*$^{83/83}$ yolk sacs contained apo-B transcripts of the identical length (~ 14 kb); however, the apo-B mRNA level was lower in the yolk sacs from *Apob*$^{83/83}$ embryos (data not shown).

To further examine the reduced mRNA levels associated with the *Apob*^{83} allele, we used primer extension assays to compare the relative amounts of the *Apob*^{83} and *Apob*^{100} mRNA levels in the liver (n = 4), intestine (n = 2), and yolk sac (n = 2) of *Apob*$^{83/100}$ mice. The steady state levels of the *Apob*^{83} transcript were reduced by 77±2% in the liver (see Fig. 8), 75% in the intestine (Fig. 5), and 76% in the yolk sac, compared with the levels of the *Apob*^{100} transcript. In parallel experiments in *Apob*$^{83/+}$ mice, *Apob*^{83} transcripts were also reduced by 75% compared with the wild-type (*Apob*$^{+}$) transcripts (data not shown). Finding identical ratios in the *Apob*$^{83/100}$ and *Apob*$^{83/+}$ mice is consistent with our prior finding that the apo-B100–only mutation has no effect on apo-B mRNA levels (15). In an additional series of experiments, we measured the relative amounts of the *Apob*^{83} and *Apob*^{100} mRNA levels in primary hepatocytes from *Apob*$^{83/100}$ mice, both at baseline, and after inhibition of RNA transcription with actinomycin D. Interestingly, actinomycin D treatment did not perturb the relative amounts of *Apob*^{83} and *Apob*^{100} transcripts within the cell (data not shown).

To determine whether the metabolism of *Apob*^{83} pre-mRNA

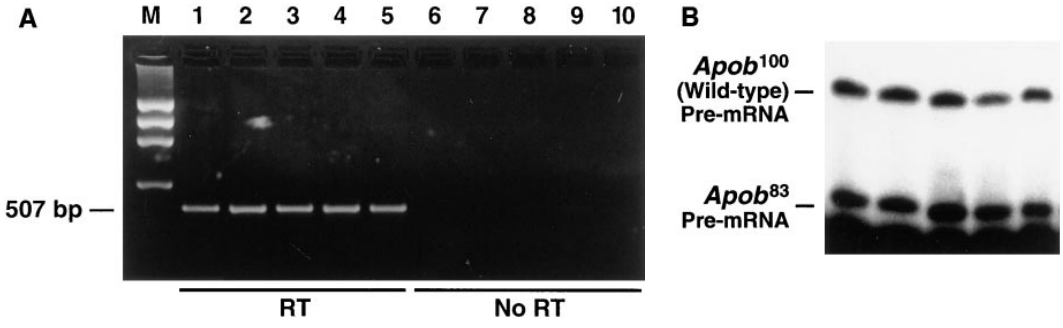

Figure 6. Primer extension analysis of enzymatically amplified apo-B pre-mRNA. (*A*) An RT-PCR reaction on liver RNA of five *Apob*$^{83/100}$ mice. Oligonucleotide primers within exon 26 and intron 26 were used to amplify unspliced mRNA from the liver RNA of *Apob*$^{83/100}$ mice. The RT-PCR product was 507 bp. No product was obtained from PCR reactions in which the reverse transcriptase step was omitted. (*B*) Primer extension assay on the RT-PCR products from the livers of five *Apob*$^{83/100}$ mice.

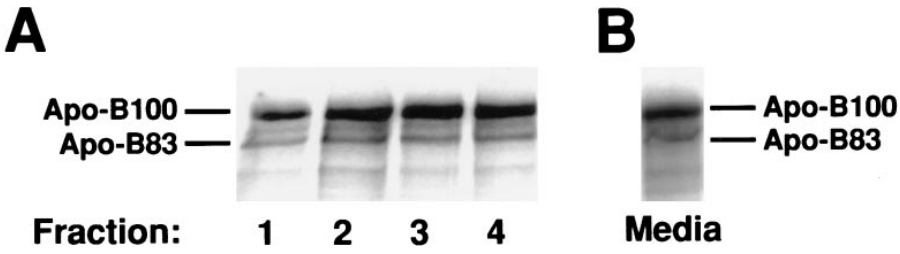

Figure 7. Secretion of apo-B83 by primary hepatocytes from *Apob*$^{83/100}$ mice. After primary hepatocytes were incubated with [^{35}S]methionine, the medium was fractionated by discontinuous sucrose gradient ultracentrifugation. The apo-B proteins were then immunoprecipitated from each fraction, and the immune complexes were fractionated by SDS-PAGE. (*A*) The VLDL/IDL fractions from the discontinuous sucrose gradient ultracentrifugation; (*B*) an unfractionated cell culture medium. Compared with apo-B100, the amount of apo-B83 secreted was reduced by ~ 75%, as judged by PhosphorImager and scanning densitometer analysis. Similar results were obtained in two additional experiments.

was altered, we quantified the relative amounts of *Apob*^{83} and *Apob*^{100} pre-mRNAs. RNA from the livers of *Apob*$^{83/100}$ mice ($n = 5$) was treated with DNase and then reverse transcribed. A 507-bp segment of the pre-mRNA was enzymatically amplified and analyzed by primer extension assay. The absence of genomic DNA contamination was documented by the inability to amplify the 507-bp DNA fragment from RNA in the absence of the reverse transcription step (Fig. 6 *A*). This analysis showed that the steady state levels of hepatic *Apob*^{83} pre-mRNA levels were slightly but significantly higher ($P < 0.01$) than the *Apob*^{100} pre-mRNA levels (the ratio of *Apob*^{83} to *Apob*^{100} pre-mRNA in five *Apob*$^{83/100}$ mice was 1.16±0.04; Fig. 6 *B*).

Production of apo-B from the Apob^{83} *and Apob*^{100} *alleles.* To assess the amount of the truncated apo-B produced and secreted by hepatocytes, we prepared primary hepatocytes from *Apob*$^{83/100}$ mice ($n = 3$) and performed [^{35}S]methionine-metabolic labeling/immunoprecipitation experiments. Compared with apo-B100, the amount of apo-B83 in *Apob*$^{83/100}$ hepatocyte lysates was reduced by 60±12% (data not shown), as judged by PhosphorImager analysis. The amount of apo-B83 in unfractionated cell culture medium was reduced by 72±5% (Fig. 7 *B*). Similar results were obtained when the autoradiographs were analyzed with a scanning densitometer. Fractionation of the cell culture media revealed that the majority of the apo-B83, like apo-B100, was secreted as VLDL/IDL (Fig. 7 *A*). As judged by densitometer analysis, the apo-B83 band in each of the VLDL/IDL fractions was ~ 25% as much as the apo-B100 band. The fact that the amount of apo-B83 in the plasma of *Apob*$^{83/100}$ was only ~ 2% of that of apo-B100 (Figs. 3 and 4), despite hepatocyte synthesis and secretion rates that were ~ 25–30% of normal, strongly suggested that apo-B83 must be removed rapidly from the plasma of *Apob*$^{83/100}$ mice.

Apo-B83 is cleared from plasma more rapidly than apo-B100. To confirm that significant amounts of apo-B83 are secreted in vivo and to assess whether the apo-B83–containing lipoproteins are cleared from plasma rapidly, we analyzed the relative amounts of apo-B83 and apo-B100 in *Apob*$^{83/100}$ mice at baseline and again after the clearance of lipoproteins from the plasma was blocked with the detergent, Triton WR-1339. For these studies, the relative amounts of apo-B83 and apo-B100 in the plasma was judged by Western blots of plasma. Before injection of Triton WR-1339, apo-B83 was not detectable in the plasma. However, increasing amounts of apo-B83 (compared with apo-B100) were observed in the plasma after the administration of Triton WR-1339 (Fig. 8). Thus, blocking the clearance of the plasma lipoproteins results in a significant enrichment of apo-B83 in the plasma, relative to apo-B100, indicating that in the setting of normal clearance mechanisms (i.e., the absence of Triton WR-1339), apo-B83 is cleared much more rapidly than apo-B100.

Apo-E and the LDL receptor are important for the rapid clearance of apo-B83. To assess what roles apo-E and the LDL receptor play in the clearance of apo-B83 compared with apo-B100, we generated *Apob*$^{83/100}$*Apoe*$^{-/-}$ and *Apob*$^{83/100}$ *Ldlr*$^{-/-}$ mice. In both *Apob*$^{83/100}$*Apoe*$^{-/-}$ ($n = 3$) and *Apob*$^{83/100}$ *Ldlr*$^{-/-}$ ($n = 4$) mice, apo-B83 was readily detectable in plasma by Western blot analysis, whereas apo-B83 could not be detected in plasma of an *Apob*$^{83/100}$ ($n = 3$; Fig. 9). The larger amount of apo-B83 (relative to apo-B100) in the *Apob*$^{83/100}$ *Apoe*$^{-/-}$ and *Apob*$^{83/100}$*Ldlr*$^{-/-}$ mice (compared with the *Apob*$^{83/100}$ mice) indicates that apo-B83 is normally cleared more rapidly than apo-B100, and that both apo-E and the LDL receptor play roles in the rapid clearance of apo-B83.

Embryonic/perinatal lethality in apo-B83–only homozygotes. Reduced apo-B synthesis and secretion was associated with developmental abnormalities in homozygous apo-B knockout mice (14, 16, 34) and homozygous apo-B70 mice (13, 35). To determine if homozygous apo-B83–only mice would manifest similar developmental defects, we intercrossed *Apob*$^{83/+}$ mice and examined the genotypes of the offspring at weaning (~ 21 d after birth). From 20 litters, we identified 102

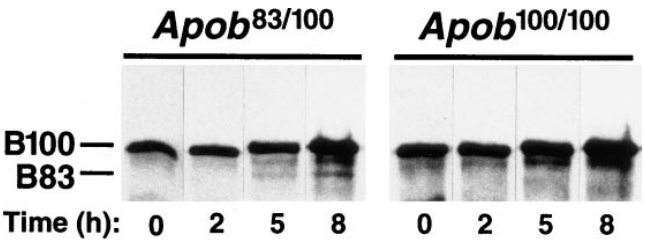

Figure 8. Inhibition of lipoprotein clearance in *Apob*$^{83/100}$ mice. The clearance of lipoproteins from the plasma of *Apob*$^{83/100}$ mice was inhibited in vivo with Triton WR-1339. Blood was collected at several time points after injection. Before Triton WR-1339 injection, Western blot analysis of plasma revealed no apo-B83; however, after administration of Triton WR-1339, increasing amounts of apo-B83, relative to apo-B100, were apparent. Results from a single *Apob*$^{83/100}$ mouse are shown. Identical results were obtained in another *Apob*$^{83/100}$ mouse in a subsequent experiment.

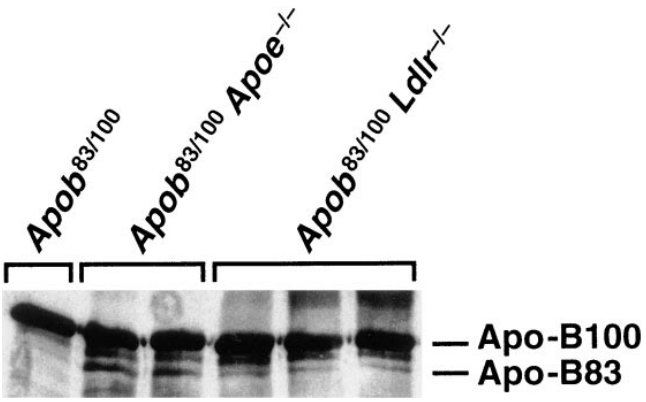

Figure 9. Rapid clearance of apo-B83 through apo-E– and LDL receptor–mediated pathways. Western blot analysis revealed that apo-B83 was readily detectable in the plasma of $Apob^{83/100}Apoe^{-/-}$ ($n = 2$) and $Apob^{83/100}Ldlr^{-/-}$ ($n = 3$) mice, but not in the plasma of $Apob^{83/100}$ controls. Identical results were obtained in several additional experiments.

Table I.

Age	Litters	$Apob^{+/+}$	$Apob^{83/+}$	$Apob^{83/83}$	Resorbed
10.5 p.c.	1	2	6	4	0
12.5 p.c.	1	4	3	5	0
14.5 p.c.	2	7	6	2 (1)‡	4
15.5 p.c.	2	3	9	4 (2)‡	7
16.5 p.c.	1	4	6	2 (1)‡	1
18.5 p.c.	1	0	7	1 (1)‡	1
20.5 p.c.	1	1	8	3 (3)‡	0
Totals (after birth)		21	45	21 (8)‡	13
Day 1–3	3	5	8	4*	
Day 21	20	44	102	0	

*Two pups were stillborn, and two pups were eaten by their mother on day 2. ‡Number of embryos manifesting gross pathology including exencephalus, herniation of the liver into the umbilical cord, bloody amniotic fluid, and/or death.

$Apob^{83/+}$ and 44 $Apob^{+/+}$ mice, but there were no $Apob^{83/83}$ mice. To further explore the absence of $Apob^{83/83}$ offspring, timed pregnancies of $Apob^{83/+}$ mice were established, and embryos were genotyped by Southern blot analysis (data not shown) and examined at gestational time points ranging from 10.5 to 20.5 days p.c. Interestingly, when the results from each of the time points were combined, $Apob^{83/83}$ embryos were identified at the expected Mendelian frequency (Table I). The majority of $Apob^{83/83}$ embryos, however, exhibited developmental abnormalities, including exencephalus, hemorrhage from the brain into the amniotic fluid, growth retardation, or herniation of the liver into the umbilical cord (Table I and Fig. 10). These abnormalities were never observed in $Apob^{83/+}$ or $Apob^{+/+}$ offspring. Microscopic analysis of $Apob^{83/83}$ embryos confirmed the presence of liver herniation and exencephalus. Because several viable homozygotes were identified during late gestation, we genotyped several newborn litters (day 1–3) from $Apob^{83/+}$ intercrosses. Two homozygotes were born alive, but both were eaten by their mother during the first 48 h of life (Table I). A single $Apob^{83/83}$ mouse, which was grossly normal in appearance, was identified at 19 d of age, but died on day 20 before blood was sampled.

Discussion

During the past 10 yr, dozens of point mutations causing truncated apo-B's and FHβ have been defined, and with each of these mutations, the plasma levels of the truncated apo-B have been very low (1). To define the cellular and molecular mechanisms for the low apo-B levels in FHβ, we used gene targeting in mouse ES cells to generate a mouse with a point mutation in the apo-B gene that resulted in the synthesis of a truncated apo-B, apo-B83. This targeted mutation produced a phenotype identical to that in humans with FHβ: low plasma levels of the apo-B–containing lipoproteins and remarkably low plasma levels of the truncated apo-B. This new gene-targeted mouse model has enabled us to examine, for the first time, how a nonsense mutation in the coding sequences of the apo-B gene affects the level of the apo-B mRNA and the levels of apo-B synthesis and secretion by the liver.

In mice carrying the apo-B83 mutation, the secretion of the truncated apo-B from hepatocytes was reduced by ~ 75%, in parallel with a virtually identical reduction in the levels of the mutant apo-B mRNA. However, the extremely low levels of the truncated apo-B in the plasma (~ 2%) were strikingly disproportional to the amount synthesized and secreted by hepatocytes (~ 25%). This observation led us to suspect that apo-B83 must be cleared from the plasma significantly more rapidly than apo-B100. This suspicion was confirmed when we examined the plasma levels of apo-B83, relative to apo-B100, in $Apob^{83/100}$ mice under experimental conditions in which lipoprotein clearance was inhibited, either pharmacologically (Triton WR-1339) or genetically (apo-E or LDL receptor deficiency). Thus, two different mechanisms—low synthesis and rapid clearance—contributed to the remarkably low levels of apo-B83 in the plasma of mice carrying the apo-B83 mutation.[3]

In our studies, the ~ 75% reduction in $Apob^{83}$ mRNA levels was documented by performing a direct comparison of the amount of $Apob^{83}$ mRNA with the amounts of $Apob^{100}$ or wild-type apo-B mRNAs. Although there are a number of precedents for low mRNA levels associated with nonsense mutations (36–39), reduced $Apob^{83}$ mRNA levels were somewhat unexpected, inasmuch as apo-B mRNA levels were normal in apo-B48–only mice, which were generated by inserting a TGA stop codon into the apo-B48–editing codon within exon 26 (15). It seems possible that mRNA levels are maintained when the nonsense mutation is placed into a physiologically normal site, whereas mutations at unnatural sites may result in reduced mRNA levels.

The relative levels of $Apob^{83}$ versus $Apob^{100}$ mRNA in $Apob^{83/100}$ primary hepatocytes remained perfectly constant

3. We believe that it is quite possible that mechanisms for hypobetalipoproteinemia could be different with mutations at other sites in the apo-B gene. For example, some mutations might decrease apo-B synthesis rates but have little effect on lipoprotein clearance.

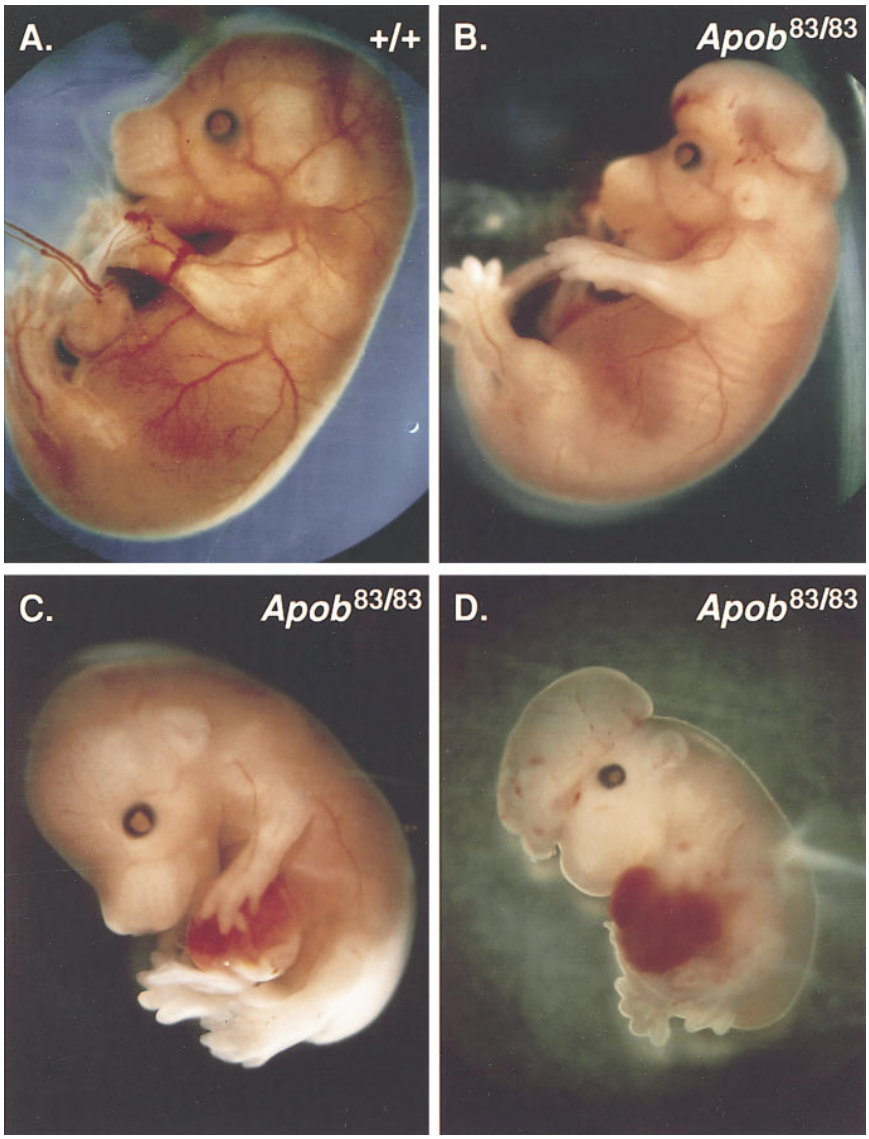

Figure 10. Developmental abnormalities in *Apob*$^{83/83}$ embryos. (*A*) A normal mouse embryo at 16.5 d p.c. (*B–D*) *Apob*$^{83/83}$ embryos at 16.5 d p.c. The embryos in *B* and *D* have exencephalus. The embryos in *C* and *D* have herniation of the liver into the umbilical cord. The embryos in panels *A–C* were derived from the same pregnancy.

over a 24-h period of transcription inhibition with actinomycin D. Although this observation suggests that the stability of cytoplasmic *Apob*^{83} mRNA may not be reduced, it is important to be cautious about the interpretation of this type of experiment, since actinomycin D can have a paradoxical effect of stabilizing specific mRNAs (36). Therefore, other mechanisms (i.e., alterations in *Apob*^{83} pre-mRNA metabolism, nuclear *Apob*^{83} mRNA metabolism, and nuclear export) could play a role in the reduced steady state levels of *Apob*^{83} mRNA.

Both apo-B100 and apo-B83 are secreted on large VLDL particles. However, the majority of apo-B100 in mouse plasma resides in the LDL, while apo-B83 is virtually undetectable in the LDL. There are several potential explanations for these findings. One is that apo-B83–containing lipoproteins, like apo-B48–containing lipoproteins, accommodate more apo-E, leading to a more rapid clearance from the plasma. However, it is unlikely that this mechanism represents the whole story because significant amounts of apo-B48 are normally present in mouse LDL (21). A second explanation is that the truncation of the apo-B molecule enhances lipoprotein binding to the LDL receptor. Schonfeld's group has previously suggested that LDL containing a long truncated apo-B (such as apo-B83) might have enhanced binding to the LDL receptor (4). In addition to enhanced binding of LDL, we speculate that the apo-B83 mutation might lead to enhanced binding of VLDL to the LDL receptor. It is widely believed that the apo-B100 molecule on VLDL particles is not in the proper conformation for binding to the LDL receptor and attains the suitable conformation only after metabolic processing to LDL (40). We suggest that apo-B83–containing VLDL might be perfectly capable of binding to the LDL receptor, which explains why this protein is cleared without metabolic processing to LDL. Indeed, it seems possible that many newly secreted apo-B83–containing VLDL are actually taken up within the Space of Disse before entering the bloodstream.

The lethal abnormalities in the homozygous *Apob*$^{83/83}$ embryos, which were similar to but less severe than those reported in homozygous apo-B–knockout mice (14, 16, 34), underscore the critical role of apo-B synthesis in mouse development. It is noteworthy that both the apo-B70 mice (which

synthesize both apo-B48 and apo-B70) (13) and the apo-B83–only mice manifested developmental abnormalities in the setting of quarter-normal levels of apo-B mRNA and apo-B synthesis, suggesting that this amount may fall below a threshold required for mouse development. The abnormalities we observed are also similar to those in vitamin E–deficient rat embryos (41–43) and therefore might be caused by a deficiency in this fat-soluble vitamin.

Acknowledgments

We thank R. Farese for RF8 ES cells; A. Garg for the plasma sample from a human subject with FHβ who was heterozygous for an apo-B83 mutation; E. Sande for performing some of the ES cell microinjections; J. Borén for advice with cell culture and metabolic labeling/immunoprecipitation experiments; J. Carroll, M. McCarthy, and A. Corder for graphics; and S. Ordway and G. Howard for reviewing the manuscript.

This work was supported by National Institutes of Health grant HL41633.

References

1. Linton, M.F., R.V. Farese, Jr., and S.G. Young. 1993. Familial hypobetalipoproteinemia. *J. Lipid Res.* 34:521–541.

2. Young, S.G., S.T. Hubl, R.S. Smith, S.M. Snyder, and J.F. Terdiman. 1990. Familial hypobetalipoproteinemia caused by a mutation in the apolipoprotein B gene that results in a truncated species of apolipoprotein B (B-31). A unique mutation that helps to define the portion of the apolipoprotein B molecule required for the formation of buoyant, triglyceride-rich lipoproteins. *J. Clin. Invest.* 85:933–942.

3. Krul, E.S., R.D. Wagner, K.G. Parhofer, H. Barrett, and G. Schonfeld. 1991. Apolipoprotein B-75: A truncated form of apolipoprotein B with increased affinity for the LDL receptor. *Circulation.* 84:II–340 (Abstr.)

4. Krul, E.S., M. Kinoshita, P. Talmud, S.E. Humphries, S. Turner, A.C. Goldberg, K. Cook, E. Boerwinkle, and G. Schonfeld. 1989. Two distinct truncated apolipoprotein B species in a kindred with hypobetalipoproteinemia. *Arteriosclerosis.* 9:856–868.

5. Parhofer, K.G., A. Daugherty, M. Kinoshita, and G. Schonfeld. 1990. Enhanced clearance from plasma of low density lipoproteins containing a truncated apolipoprotein, apoB-89. *J. Lipid Res.* 31:2001–2007.

6. Parhofer, K.G., P.H.R. Barrett, D.M. Bier, and G. Schonfeld. 1991. Determination of kinetic parameters of apolipoprotein B metabolism using amino acids labeled with stable isotopes. *J. Lipid Res.* 32:1311–1323.

7. Krul, E.S., K.G. Parhofer, P.H.R. Barrett, R.D. Wagner, and G. Schonfeld. 1992. ApoB-75, a truncation of apolipoprotein B associated with familial hypobetalipoproteinemia: genetic and kinetic studies. *J. Lipid Res.* 33:1037–1050.

8. Parhofer, K.G., P.H.R. Barrett, D.M. Bier, and G. Schonfeld. 1992. Lipoproteins containing the truncated apolipoprotein, apo B-89, are cleared from human plasma more rapidly than apo B-100–containing lipoproteins in vivo. *J. Clin. Invest.* 89:1931–1937.

9. Barrett, P.H.R., K.G. Parhofer, S.G. Young, and G. Schonfeld. 1992. Apolipoproteins B-31 and B-54.8: truncations associated with reduced apoB production rates. *Circulation.* 86:I–209 (Abstr.)

10. Srivastava, N., D. Noto, M. Averna, J. Pulai, R.A.K. Srivastava, T.G. Cole, M.A. Latour, B.W. Patterson, and G. Schonfeld. 1996. A new apolipoprotein B truncation (apo B-43.7) in familial hypobetalipoproteinemia: genetic and metabolic studies. *Metab. Clin. Exp.* 45:1296–1304.

11. Parhofer, K.G., P.H.R. Barrett, C.A. Aguilar-Salinas, and G. Schonfeld. 1996. Positive linear correlation between the length of truncated apolipoprotein B and its secretion rate: in vivo studies in human apoB-89, apoB-75, apoB-54.8, and apoB-31 heterozygotes. *J. Lipid Res.* 37:844–852.

12. Grundy, S.M., and G.L. Vega. 1991. What is meant by overproduction of apo B–containing lipoproteins? *Adv. Exp. Med. Biol.* 285:213–222.

13. Homanics, G.E., T.J. Smith, S.H. Zhang, D. Lee, S.G. Young, and N. Maeda. 1993. Targeted modification of the apolipoprotein B gene results in hypobetalipoproteinemia and developmental abnormalities in mice. *Proc. Natl. Acad. Sci. USA.* 90:2389–2393.

14. Farese, R.V., Jr., S.L. Ruland, L.M. Flynn, R.P. Stokowski, and S.G. Young. 1995. Knockout of the mouse apolipoprotein B gene results in embryonic lethality in homozygotes and protection against diet-induced hypercholesterolemia in heterozygotes. *Proc. Natl. Acad. Sci. USA.* 92:1774–1778.

15. Farese, R.V., Jr., M.M. Véniant, C.M. Cham, L.M. Flynn, V. Pierotti, J.F. Loring, M. Traber, S. Ruland, R.S. Stokowski, D. Huszar, and S.G. Young. 1996. Phenotypic analysis of mice expressing exclusively apolipoprotein B48 or apolipoprotein B100. *Proc. Natl. Acad. Sci. USA.* 93:6393–6398.

16. Huang, L.-S., E. Voyiaziakis, D.F. Markenson, K.A. Sokol, T. Hayek, and J.L. Breslow. 1995. Apo B gene knockout in mice results in embryad neural tube defects, male infertility, and reduced HDL cholesterol ester and apo A-I transport rates in heterozygotes. *J. Clin. Invest.* 96:2152–2161.

17. Hogan, B., R. Beddington, F. Costantini, and E. Lacy. 1994. Manipulating the Mouse Embryo. A Laboratory Manual. Cold Spring Harbor Laboratory Press, Plainview, NY. 128–252.

18. Piedrahita, J.A., S.H. Zhang, J.R. Hagaman, P.M. Oliver, and N. Maeda. 1992. Generation of mice carrying a mutant apolipoprotein E gene inactivated by gene targeting in embryonic stem cells. *Proc. Natl. Acad. Sci. USA.* 89:4471–4475.

19. Zhang, S.H., R.L. Reddick, J.A. Piedrahita, and N. Maeda. 1992. Spontaneous hypercholesterolemia and arterial lesions in mice lacking apolipoprotein E. *Science.* 258:468–471.

20. Ishibashi, S., M.S. Brown, J.L. Goldstein, R.D. Gerard, R.E. Hammer, and J. Herz. 1993. Hypercholesterolemia in low density lipoprotein receptor knockout mice and its reversal by adenovirus-mediated gene delivery. *J. Clin. Invest.* 92:883–893.

21. McCormick, S.P.A., J.K. Ng, M. Véniant, J. Borén, V. Pierotti, L.M. Flynn, D.S. Grass, A. Connolly, and S.G. Young. 1996. Transgenic mice that overexpress mouse apolipoprotein B. Evidence that the DNA sequences controlling intestinal expression of the apolipoprotein B gene are distant from the structural gene. *J. Biol. Chem.* 271:11963–11970.

22. Farese, R.V., Jr., A. Garg, V.R. Pierotti, G.L. Vega, and S.G. Young. 1992. A truncated species of apolipoprotein B, B-83, associated with hypobetalipoproteinemia. *J. Lipid Res.* 33:569–577.

23. Marcel, Y.L., M. Hogue, R. Theolis, Jr., and R.W. Milne. 1982. Mapping of antigenic determinants of human apolipoprotein B using monoclonal antibodies against low density lipoproteins. *J. Biol. Chem.* 257:13165–13168.

24. Pease, R.J., R.W. Milne, W.K. Jessup, A. Law, P. Provost, J.-C. Fruchart, R.T. Dean, Y.L. Marcel, and J. Scott. 1990. Use of bacterial expression cloning to localize the epitopes for a series of monoclonal antibodies against apolipoprotein B100. *J. Biol. Chem.* 265:553–568.

25. Linton, M.F., R.V. Farese, Jr., G. Chiesa, D.S. Grass, P. Chin, R.E. Hammer, H.H. Hobbs, and S.G. Young. 1993. Transgenic mice expressing high plasma concentrations of human apolipoprotein B100 and lipoprotein(a). *J. Clin. Invest.* 92:3029–3037.

26. McCormick, S.P.A., M.F. Linton, H.H. Hobbs, S. Taylor, L.K. Curtiss, and S.G. Young. 1994. Expression of human apolipoprotein B90 in transgenic mice. Demonstration that apolipoprotein B90 lacks the structural requirements to form lipoprotein(a). *J. Biol. Chem.* 269:24284–24289.

27. Purcell-Huynh, D.A., R.V. Farese, Jr., D.F. Johnson, L.M. Flynn, V. Pierotti, D.L. Newland, M.F. Linton, D.A. Sanan, and S.G. Young. 1995. Transgenic mice expressing high levels of human apolipoprotein B develop severe atherosclerotic lesions in response to a high-fat diet. *J. Clin. Invest.* 95:2246–2257.

28. McCormick, S.P.A., J.K. Ng, S. Taylor, L.M. Flynn, R.E. Hammer, and S.G. Young. 1995. Mutagenesis of the human apolipoprotein B gene in a yeast artificial chromosome reveals the site of attachment for apolipoprotein(a). *Proc. Natl. Acad. Sci. USA.* 92:10147–10151.

29. Nielsen, L.B., S.P.A. McCormick, V. Pierotti, C. Tam, M.D. Gunn, H. Shizuya, and S.G. Young. 1997. Human apolipoprotein B transgenic mice generated with 207-kb and 145-kb bacterial artificial chromosomes: Evidence that a distant 5′ element confers appropriate transgene expression in the intestine. *J. Biol. Chem.* 272:29752–29758.

30. Véniant, M.M., V. Pierotti, D. Newland, C.M. Cham, D.A. Sanan, R.L. Walzem, and S.G. Young. 1997. Susceptibility to atherosclerosis in mice expressing exclusively apolipoprotein B48 or apolipoprotein B100. *J. Clin. Invest.* 100:180–188.

31. Seglen, P.O. 1973. Preparation of rat liver cells. II. Effects of ions and chelators on tissue dispersion. *Exp. Cell Res.* 76:25–30.

32. Borén, J., S. Rustaeus, and S.-O. Olofsson. 1994. Studies on the assembly of apolipoprotein B-100– and B-48–containing very low density lipoproteins in McA-RH7777 cells. *J. Biol. Chem.* 269:25879–25888.

33. Li, X., F. Catalina, S.M. Grundy, and S. Patel. 1996. Method to measure apolipoprotein B-48 and B-100 secretion rates in an individual mouse: evidence for a very rapid turnover of VLDL and preferential removal of B-48–relative to B-100–containing lipoproteins. *J. Lipid Res.* 37:210–220.

34. Farese, R.V., Jr., S. Cases, S.L. Ruland, H.J. Kayden, J.S. Wong, S.G. Young, and R.L. Hamilton. 1996. A novel function for apolipoprotein B: lipoprotein synthesis in the yolk sac is critical for maternal–fetal lipid transport in mice. *J. Lipid Res.* 37:347–360.

35. Homanics, G.E., N. Maeda, M.G. Traber, H.J. Kayden, D.B. Dehart, and K.K. Sulik. 1995. Exencephaly and hydrocephaly in mice with targeted modification of the apolipoprotein B (*Apob*) gene. *Teratology.* 51:1–10.

36. Kessler, O., and L.A. Chasin. 1996. Effects of nonsense mutations on nuclear and cytoplasmic adenine phosphoribosyltransferase RNA. *Mol. Cell. Biol.* 16:4426–4435.

37. Maquat, L.E. 1995. When cells stop making sense: effects of nonsense codons on RNA metabolism in vertebrate cells. *RNA (NY).* 1:453–465.

38. Baserga, S.J., and E.J. Benz, Jr. 1988. Nonsense mutations in the human β-globin gene affect mRNA metabolism. *Proc. Natl. Acad. Sci. USA.* 85:2056–2060.

39. Baserga, S.J., and E.J. Benz, Jr. 1992. β-globin nonsense mutation: deficient accumulation of mRNA occurs despite normal cytoplasmic stability. *Proc. Natl. Acad. Sci. USA.* 89:2935–2939.

40. Krul, E.S., M.J. Tikkanen, T.G. Cole, J.M. Davie, and G. Schonfeld. 1985. Roles of apolipoproteins B and E in the cellular binding of very low density lipoproteins. *J. Clin. Invest.* 75:361–369.

41. Verma, K., and D.W. King. 1967. Disorders of the developing nervous system of vitamin E–deficient rats. *Acta Anat.* 67:623–635.

42. Cheng, D.W., L.F. Chang, and T.A. Bairnson. 1957. Gross observations on developing abnormal embryos induced by maternal vitamin E deficiency. *Anat. Rec.* 129:167–185.

43. Urner, J.A. 1931. The intra-uterine changes in the pregnant albino rat (Mus norvegicus) deprived of vitamin E. *Anat. Rec.* 50:175–187.